American Journal of Pathology, Vol. 166, No. 1, January 2005

Immunopathology and Infectious Disease

Enhanced Susceptibility to Endotoxic Shock and Impaired STAT3 Signaling in CD31-Deficient Mice

Michael Carrithers,* Suman Tandon,† Sandra Canosa,† Michael Michaud,† Donnasue Graesser,† and Joseph A. Madri†

From the Department of Neurology, Section of Immunobiology, and Department of Pathology,† Yale University School of Medicine, New Haven, Connecticut*

Platelet endothelial cell adhesion molecule-1 (PECAM-1, CD31), an adhesion molecule expressed on hematopoietic and endothelial cells, mediates apoptosis, cell proliferation, and migration and maintains endothelial integrity in addition to its roles as a modulator of lymphocyte and platelet signaling and facilitator of neutrophil transmigration. Recent data suggest that CD31 functions as a scaffolding protein to regulate phosphorylation of the signal transducers and activators of transcription (STAT) family of signaling molecules, particularly STAT3 and STAT5. STAT3 regulates the acute phase response to innate immune stimuli such as lipopolysaccharide (LPS) and promotes recovery from LPS-induced septic shock. Here we demonstrate that CD31-deficient mice have reduced survival during endotoxic LPS-induced shock. As compared to wild-type controls, CD31-deficient mice showed enhanced vascular permeability; increased apoptotic cell death in liver, kidney, and spleen; and elevated levels of serum tumor necrosis factor α (TNF-α), interferon γ (IFNγ), MCP-1, MCP-5, sTNRF, and IL-6. In response to LPS *in vivo* and *in vitro*, splenocytes and endothelial cells from knockout mice had reduced levels of phosphorylated STAT3. These results suggest that CD31 is necessary for maintenance of endothelial integrity and prevention of apoptosis during septic shock and for STAT3-mediated acute phase responses that promote survival during septic shock. *(Am J Pathol 2005, 166:185–196)*

Platelet endothelial cell adhesion molecule-1 (PECAM-1, CD31) belongs to the immunoglobulin family of cell adhesion molecules.[1–3] CD31 mediates homophilic and heterophilic binding in hematopoietic and endothelial cells and also modulates intracellular signaling.[4–10]

CD31-mediated adhesion enhances transendothelial migration of leukocytes to sites of acute inflammation.[11] Recent work also suggests that homophilic CD31 binding between endothelial cells maintains vascular integrity and prevents prolonged changes in permeability.[12] Cultured endothelial cells from CD31-deficient mice demonstrate enhanced transendothelial migration of T lymphocytes and prolonged permeability changes in response to histamine. In experimental autoimmune encephalomyelitis (EAE), the animal model of human multiple sclerosis, CD31-deficient mice develop earlier onset of disease due to enhanced migration of immune cells into the brain and spinal cord.

CD31 regulation of intracellular signaling occurs through recruitment of adapter and signaling molecules to an immunoreceptor tyrosine activation motif (ITAM) on the cytoplasmic domain of CD31.[6–10] By serving a scaffolding function, it has been hypothesized that CD31 mediates tyrosine phosphorylation of two members of the STAT (signal transducers and activators of transcription) family, STAT3 and STAT5.[8] Based on its multiple roles in cell adhesion, leukocyte migration, and cell signaling, we reasoned that CD31 would also regulate the acute phase response (APR). Either infection or tissue injury can trigger the APR.[13] In acute infection, binding of pathogen-associated molecular patterns (PAMPs) such as lipopolysaccharide (LPS) on gram-negative bacteria and lipotechoic acids on gram-positive bacteria to the Toll-like family of pattern recognition receptors initiates the APR.[14] Although this innate immune response is necessary to host survival during severe infection, impaired regulation of the APR can lead to septic shock.[15] For example, activation of Toll receptors on macrophages and other immune cells leads to local release of pro-

Supported in part by United States Public Health Service Grants R37-HL28373, RO1-HL51018, PO1-DK55389 (to J.A.M.), K08 NS02124–01 (to M.D.C.), and by a Dana Foundation Award in "Clinical Hypotheses in Neuroimmunology" (to M.D.C.).

M.C., S.T., and S.C. contributed equally to this manuscript.

Accepted for publication October 1, 2004.

Address reprint requests to Joseph A. Madri, M.D., Ph.D., Department of Pathology, Yale University School of Medicine, 310 Cedar Street, New Haven, CT 06520. E-mail: joseph.madri@yale.edu.

inflammatory cytokines such as interleukin 6 (IL-6).[16] IL-6 and related cytokines signal through phosphorylation of the transcription factor, STAT3.[17,18] During the APR, phosphorylated STAT3 (pSTAT3) stimulates transcription of pro- and anti-inflammatory molecules. In cell-specific gene knockout models, STAT3 deficiency in hepatocytes impairs the APR to LPS, and, in mice with STAT3-deficient monocytes and neutrophils, there is reduced survival from endotoxic shock.[19,20]

We hypothesized that CD31 maintenance of endothelial integrity and regulation of phosphorylation of STAT3 enhance recovery from endotoxic shock. We here show that CD31-deficient mice are markedly more sensitive to LPS-induced shock as compared to wild-type (WT) mice. In response to LPS, these mice demonstrate reduced survival, increased vascular permeability and apoptosis in solid organs, elevated serum TNF-α, IFNγ, MCP-1, MCP-5, sTNFR1, and IL-6 and decreased levels of phosphorylated STAT3.

Materials and Methods

Mice

Female C57Bl/6CR mice (6 to 8 weeks of age) were obtained from Charles River Laboratories (Wilmington, MA). CD31-deficient mice on the C57Bl/6CR background were generated and analyzed as described previously.[12,21] They were bred in our facility at Yale University and have been backcrossed onto the C57Bl6 background for greater than 10 generations.[12]

LPS-Induced Endotoxic Shock

LPS (*E. coli* serotype 055:B5; Sigma Chemical Co., St. Louis, MO) was administered intraperitoneally (i.p.) at doses of 200 μg or 600 μg per mouse in 200 μl phosphate-buffered saline (PBS). Control mice received PBS. Clinical status was monitored twice daily for 7 days.

Vascular Permeability

One day after a 200-μg dose of LPS, Evans blue dye was injected intravenously. One hour later, mice were anesthetized with ketamine/xylazine, and intracardiac perfusion was performed with ice-cold PBS. Lung, liver, and kidney were isolated, and dye was extracted in formamide (5 μl/mg of tissue) for 3 days at room temperature. Absorbance at 650 nm was measured to determine dye concentration as described.[12]

Histology

Wild-type and CD31-deficient C57BL6 were injected with 200 μg of LPS i.p. One day later, mice were anesthetized with ketamine/xylazine, and intracardiac perfusion was performed with ice-cold PBS followed by paraformaldehyde-lysine-periodate (PLP) fixative. Lung, liver, and kidney were harvested and fixed in PLP overnight. Tissue was dehydrated through graded ethanol, cleared in xylene, and embedded in paraffin. Five-μm sections were stained with hematoxylin/eosin (H&E).

Cytokine Analysis

Mouse Th1/Th2 Cytokine CBA (BD Biosciences, San Jose, CA) was performed according to manufacturer's instructions (Manual No. 551287) on serum samples obtained by eye bleed from wild-type or CD31-deficient mice treated with 10 μg/g LPS for 24 hours.

ELISA for mouse TNF-α was obtained from Endogen (Endogen-Pierce mouse TNF α ELISA Minikit No. KMT-NFA) and performed according to manufacturer's instructions (Pierce Biotechnology, Inc., Rockford, IL).

Mouse Cytokine Antibody Array (Kit No. MA6060) (Panomics, Redwood City, CA) was performed on serum from mice injected with 10 μg/g LPS for 6, 12, or 24 hours, plus saline controls, according to manufacturer's instructions.

Splenocyte Cell Culture

Sex- and age-matched wild-type and CD31-deficient C57Bl6 mice were sacrificed by cervical dislocation and spleens removed under sterile conditions. Splenocytes were teased from the spleens by crushing between the frosted ends of microscope slides in sterile PBS. The resulting cell suspension was then run through a cell strainer (Falcon), spun out, and the red blood cells lysed in ACK buffer (0.15 mol/L NH_4Cl, 10 mmol/L $KHCO_3$, 0.1 mmol/L Na_2EDTA pH 7.2). Lymphocytes were then isolated by gradient centrifugation in LSM (ICN Biomedicals) and plated at 5.5×10^6 cells in 60-mm dishes. Lymphocytes were then exposed to 0, 10, and 100 ng/ml LPS (Sigma, *E. coli* serotype 055:B5) for 24 hours in Clicks Media (Irvine Scientific) supplemented with 10% fetal bovine serum (FBS), L-glutamine, pen/strep, and 2-mercaptoethanol. Cells were lysed in 20 mmol/L Tris-HCl pH 7.5, 150 mmol/L NaCl, 1 mmol/L $MgCl_2$, 1 mmol/L EGTA, 10 mmol/L $Na_4P_2O_7$, 1% Brij-35, Complete Protease Inhibitors (Roche), 5 mmol/L NaF, 250 μmol/L NaOV, and 1 mmol/L PMSF, and assayed for protein content by bicinchoninic acid (BCA) assay (Pierce Biotechnology, Inc., Rockford, IL). Twenty μg of each sample was loaded onto 8% SDS-PAGE for immunoblotting with anti-pY(705) STAT3 and anti-STAT3 (Cell Signaling, both at 1:1000 in 0.05% T-TBS plus 1% normal donkey serum, followed by anti-rabbit IgG-HRP conjugate. Signals were detected with Western Lightning Reagent (Perkin Elmer, Boston, MA) on Hyperfilm MP (Amersham/Pharmacia).

Endothelial Cell Culture

Immortalized CD31-reconstituted and CD31-deficient mouse lung endothelial cells were cultured in Dulbecco's modified Eagle's medium enriched with 10% FBS, L-glutamine, non-essential amino acids, sodium pyruvate, HEPES, and β-mercaptoethanol as described.[12] Puromy-

cin was added to the cell medium used to passage the CD31-reconstituted cultures. Cells were used between passages 16 and 22. Endothelial cell cultures were grown to confluency and then treated with LPS at concentrations of 100 and 500 ng/ml for 0.5, 2, 6, 12, and 24 hours. Untreated cells were used as controls. Cells were pretreated with 1 mmol/L sodium orthovanadate for 15 minutes at 37°C, washed twice with ice-cold PBS containing 1 mmol/L sodium orthovanadate, and scraped into ice-cold lysis buffer [50 mmol/L Tris, pH 7.4, 100 mmol/L sodium chloride, 0.5% Triton X-100, 0.5% DOC, 1 mmol/L sodium orthovanadate, and Complete Protease Inhibitor Cocktail Tablets (Roche). Total cellular protein concentration was determined by BCA assay (Pierce) according to the manufacturer's instructions. Lysates (20 μg per sample) were then subjected to immunoblot as described.

Immunoblotting

Endothelial cell culture lysates were resolved on 8% SDS-polyacrylamide gels and transferred to polyvinylidene fluoride membrane (Millipore Corp., Bedford, MA). Blots were blocked with 5% milk and then incubated overnight with anti-Py-Stat3 (Tyr 705, rabbit, 1:500) and anti-Stat3 (C 20, rabbit, 1:5000), or with anti-TLR4 (Imgenex, IMG-579A, rabbit, 1:200, San Diego, CA). After washing with 0.1% TBST, blots were incubated with horseradish peroxidase-conjugated goat anti-rabbit IgG (1:10,000) for 1 hour and washed again with 0.1% TBST. Blots were developed with enhanced chemiluminescence (Western Lightning, Perkin Elmer) and exposed to high performance autoradiography film (Amersham Pharmacia). Blots were scanned on an Arcus II scanner (Agfa, Mortsel, Belgium) and quantitated using BioMax 1D software (Kodak, Rochester, NY).

Tissue and Culture Lysates

Six wild-type C57Bl/6CR (three males, three females) and six CD31-deficient mice (three males, three females), 7 weeks old, were injected intraperitoneally with 200 μg of LPS. Animals were sacrificed 24 hours after the injection and organs harvested. 100 mg of tissue was homogenized in 2 ml of 2X Laemlli buffer (125 mmol/L Tris-HCl, pH 6.8, 4% SDS, 25% glycerol, bromophenol blue, 2% BME) containing 1 mmol/L sodium orthovanadate and protease inhibitor cocktail tablet (40 μl/ml) followed by brief sonication. After centrifugation at 14,000 rpm, the supernatant was collected. Fifteen μl of each sample was resolved on 8% SDS-polyacrylamide gels and transferred to polyvinylidene fluoride membrane (Millipore) for immunoblotting as described.

Sodium Orthovanadate Treatment

Age-matched wild-type and PECAM-1-deficient mice were sacrificed and spleens harvested. Isolated splenocytes were incubated at 37°C in the presence of 1 ng/ml IL-6 with and without 1 mmol/L sodium orthovanadate (NaOV) for 15 to 30 minutes, followed by two ice-cold PBS washes and lysis in 20 mmol/L Tris-HCl, pH 7.5, 150 mmol/L NaCl, 10 mmol/L $NA_4P_2O_4$, 1% Brij, 1 mmol/L $MgCl_2$, 1 mmol/L EGTA, 1 mmol/L PMSF, 5 mmol/L NaF, 250 μmol/L NaOV, and Complete Protease Inhibitor (Roche). Twenty μg of cell lysate were run of 8% SDS-PAGE gels, and blotted in pY-STAT3 antibody (Cell Signaling) and subsequently stripped and re-probed with SATA3 antibody (Cell Signaling) as per manufacturer's instructions. Results were analyzed using Kodak 1D software.

FACS Analysis

Splenocytes were prepared as described, fixed in 2% PFA, then stained with 0.5 μg of polyclonal anti-mouse TLR4 (Imgenex) in Hanks' buffered salt solution plus 1% BSA for 1 hour on ice, then, following two washes, in donkey anti-rabbit IgG F(ab′)2 PE conjugate (Jackson Immunoresearch, West Grove, PA). Endothelial cells were also fixed and stained in 0.5 μg of anti-TLR4 as above, but the signal was amplified with donkey anti-rabbit biotin conjugate secondary (Santa Cruz Biotechnology, Santa Cruz, CA) followed by a streptavidin PE conjugate (Caltag Laboratories, Burlingame, CA). Samples were analyzed on a BD FACScalibur flow cytometer using BD CellQuest software.

Immunofluorescence

Immortalized PECAM reconstituted and knock-out mouse lung endothelial cells were cultured in chamber slides (Lab-Tek, Nalge-Nunc International, Rochester, NY) to confluence in 0.5% culture media, then fed new 0.5% culture media for 1 hour, followed by treatment for 24 hours or 5 hours with 100 ng/ml LPS in serum-free conditions. Cell monolayers were fixed for 15 minutes in 2% PFA at room temperature, followed by three 1% BSA/PBS washes of 5 minutes each. Monolayers were extracted at 4°C for 10 minutes in 15 mmol/L Tris pH 7.5, 120 mmol/L NaCl, 25 mmol/L KCl, 2 mmol/L EDTA, 2 mmol/L EGTA, 0.1 mmol/L DTT, 0.5 mmol/L PMSF, and 0.5% Triton X-100. Following a 1-hour room temperature wash in 1% BSA/PBS plus 5.5% normal donkey serum, primary antibodies anti-STAT3 or anti-pY(705) STAT3 (both Cell Signaling at 1:500) were added and incubated overnight at 4°C. Samples were washed three more times, 5 minutes each at 4°C in 1% BSA/PBS, then incubated with Alexa Fluor 594 anti-rabbit at 1:400 for 1 hour at room temperature. After three more rounds of washes, cells were mounted in VectaShield +DAPI mounting. A similar protocol was used to label splenic tissue previously fixed with PLP and then submitted to frozen sectioning at a 5-μm thickness.

Statistics

Results were analyzed using Statview Version 5 Software (SAS Institute, Inc.) N-way analysis of variance and all pair-wise multiple comparison procedures (Fisher's PLSD, Bonferroni/Dunn, and Student-Newman-Keuls

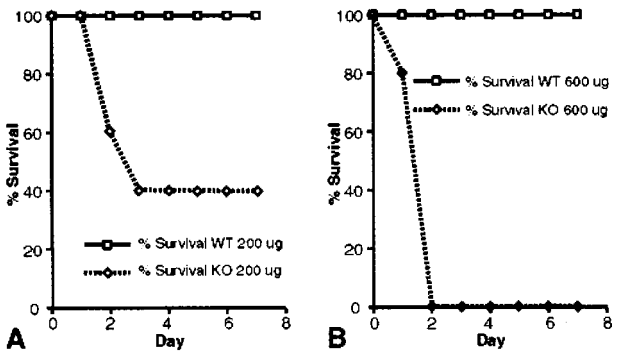

Figure 1. Decreased survival in CD31-deficient mice treated with LPS. Kaplan-Meyer curves demonstrate 100% survival of wild-type mice at two doses of LPS (*E. coli* serotype 055:B5), 200 μg (**A**) and 600 μg (**B**) ($n = 8$ for each dose). In contrast, CD31-deficient mice had 43% survival at 200 μg ($n = 7$) and 0% survival at 600 μg ($n = 8$).

methods). Alternatively, the Student's *t*-test was used. Statistical significance was defined as a *P* value of <0.05.

Results

Impaired Recovery from Endotoxic Shock in CD31-Deficient Mice

To assess the differences in response to LPS, wild-type and CD31-deficient mice were treated with 600 μg LPS (*E. coli* serotype 055:B5) and then followed for clinical signs of sepsis. This dose was chosen because it had been previously shown to be a sublethal dose in wild-type C57BL6 mice (data not shown). To our surprise, although all wild-type mice survived (8 of 8 animals), there were no survivors (0 of 8) in the CD31-deficient group 2 days following LPS administration (Figure 1B). At a lower LPS dose (200 μg), there was 43% survival in the CD31-deficient group (3 of 7) and 100% survival among wild-type animals (8 of 8) (Figure 1A).

Enhanced Vascular Permeability in Response to LPS in CD31-Deficient Mice

Our previous studies illustrated that while under baseline, un-stimulated conditions wild-type and CD31-deficient mice exhibit similar vascular permeability profiles (both exhibiting negligible Evans blue extravasation), stimulation by either initiating an inflammatory response (MOG peptide-induced EAE) or using a vasoactive agent (intradermal injection of histamine) resulted in a pronounced increase in organ/tissue-specific permeability in the CD31-deficient animals compared to their wild-type counterparts.[12] In the current study, 1 day following a 200-μg dose of LPS, vascular permeability was analyzed by the Evans Blue technique. In surviving mice, LPS treatment resulted in a greater permeability change in CD31-deficient lung, kidney, and liver as compared to wild-type controls (Table 1). These differences were statistically significant ($P < 0.005$ for lung, $P < 0.008$ kidney, and $P < 0.03$ for liver).

Table 1. Increased Vascular Permeability in CD31-Deficient Lung, Kidney, and Liver 24 Hours Following LPS Treatment (200 μg) as Determined by the Presence of Evans Blue Dye in Tissues ($OD_{650\ nm}$)

Organ	Wild-Type (Abs. at 650 nm)	CD31-Deficient (Abs. at 650 nm)
Lung	0.139 ± 0.026	$0.275 \pm 0.056^{*}$
Kidney	0.138 ± 0.018	$0.219 \pm 0.031^{\dagger}$
Liver	0.227 ± 0.024	$0.279 \pm 0.039^{\ddagger}$

*, $P < 0.005$, †, $P < 0.008$, ‡, $P < 0.03$.

In the CD31-deficient tissues, there was a significant increase (2-fold in the lung, 1.6-fold in the kidney, and 1.3-fold in the liver) in permeability following LPS treatment ($n = 6$). Abs, absorbance.

Increased Capillary Leak and Apoptosis in Multiple Organs following LPS Challenge in CD31-Deficient Mice

One day after a 200-μg dose of LPS, histological analysis was performed on lung, liver, kidney, and spleen in surviving mice. In all tissues, intense capillary leak was observed in CD31-deficient mice compared to controls. Lungs from CD31-deficient mice demonstrated vascular congestion and edema (Table 1 and Figure 2, C and F). LPS treatment did not appreciably alter lung morphology in wild-type mice (compare Figure 2, A and D with Figure 2, B and E).

Examination of the kidneys revealed glomerular and peri-tubular capillary vascular congestion as well as occasional peritubular endothelial cell karyorexis and karyolysis in CD31-deficient mice (Figure 3, C, H, I, N, and O). While LPS treatment did induce mild congestion in wild-type mice (Figure 3, B, F, G, L, and M), no evidence of karyorexis or karyolysis was evident. Confirmation of peritubular capillary endothelial cell apoptosis in CD31-deficient mice was demonstrated by TUNEL staining (Figure 4).

In the liver, vascular congestion, sinusoidal and portal inflammation was noted in the CD31-deficient mice treated with LPS (Figure 5C, F, I, and J). Wild-type mice treated with LPS demonstrated no appreciable hepatic vascular or sinusoidal congestion (Figure 5, B, E, and H) compared to untreated wild-type mice (Figure 5, A, D, and G). The congestion in CD31-deficient mice was more severe and was associated with sinusoidal and portal neutrophilic infiltration (Figure 6, I and J).

Examination of the spleens revealed increased vascular congestion of the red pulp in CD31-deficient mice following LPS treatment. While LPS treatment did induce mild congestion in wild-type mice, no evidence of karyorexis or karyolysis was evident (Figure 6, A and B). TUNEL labeling of paraffin sections of splenic tissue harvested from control (not shown) and LPS-treated (200 μg for 24 hours) WT and CD31 KO mice revealed robust increases in TUNEL-positive cells in the follicular center regions of spleens harvested from LPS-treated CD31 KO mice, while in LPS-treated WT mice only modest TUNEL labeling was noted (compare Figure 6, C and D). A and B: scale bar, 100 μm; C and D: scale bar, 50 μm.

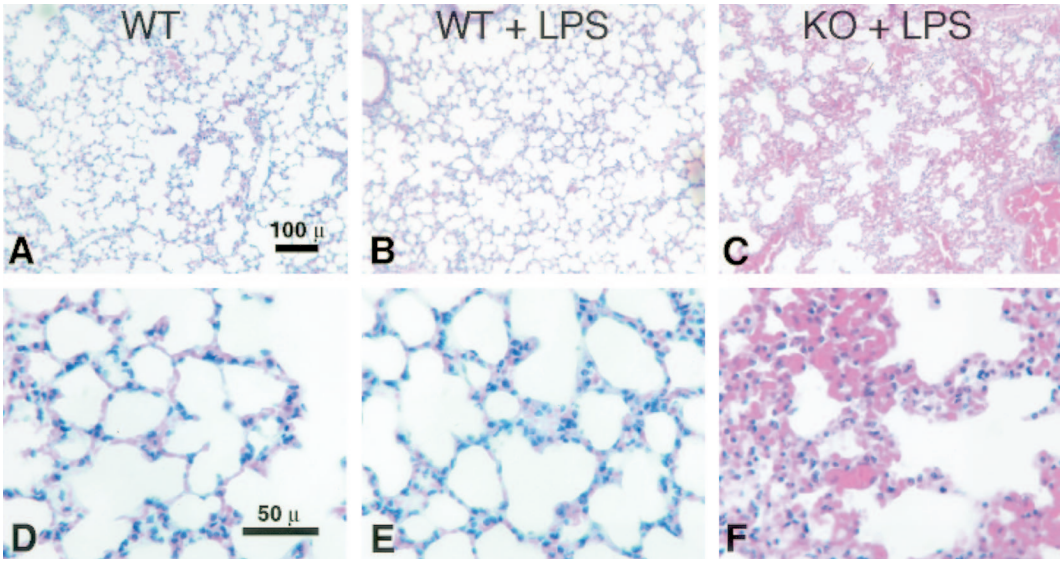

Figure 2. Pulmonary edema and congestion occur in CD31-deficient mice following LPS stimulation. Representative low- (**A–C**) and high- (**D–F**) power H&E micrographs of lungs harvested from age- and sex-matched wild-type control mice (WT), wild-type mice treated with LPS (WT + LPS), and CD31-deficient mice treated with LPS (CD31 + LPS). Lung tissue harvested from CD31-deficient mice (not shown) appeared indistinguishable from WT control mice (**A** and **D**). Treatment of WT mice with LPS resulted in no appreciable changes in lung morphology (compare **A** and **D** with **B** and **E**). In contrast, treatment of CD31-deficient mice with LPS resulted in significant vascular congestion and edema (Table 1 and **C** and **F**). **Bar**, 100 μm (**A** to **C**); **bar**, 50 μm (**D** to **F**.)

Increased Serum Cytokine Levels in LPS-Treated CD31-Deficient Mice

As expected, cytokine levels in both wild-type and CD31-deficient mice were below detectable levels before LPS treatment (Figure 7A, top two panels at the zero (0) time-point). However, 24 hours following a 200-μg dose of LPS, TNF-α levels in the serum as measured by ELISA were approximately 10-fold higher in CD31-deficient mice as compared to LPS-treated wild-type mice (Figure 7A). These results were confirmed by a BD cytometric bead assay (not shown). This finding prompted us to examine the serum expression levels of other cytokines and chemokines known to be dynamically regulated using inflammatory responses.

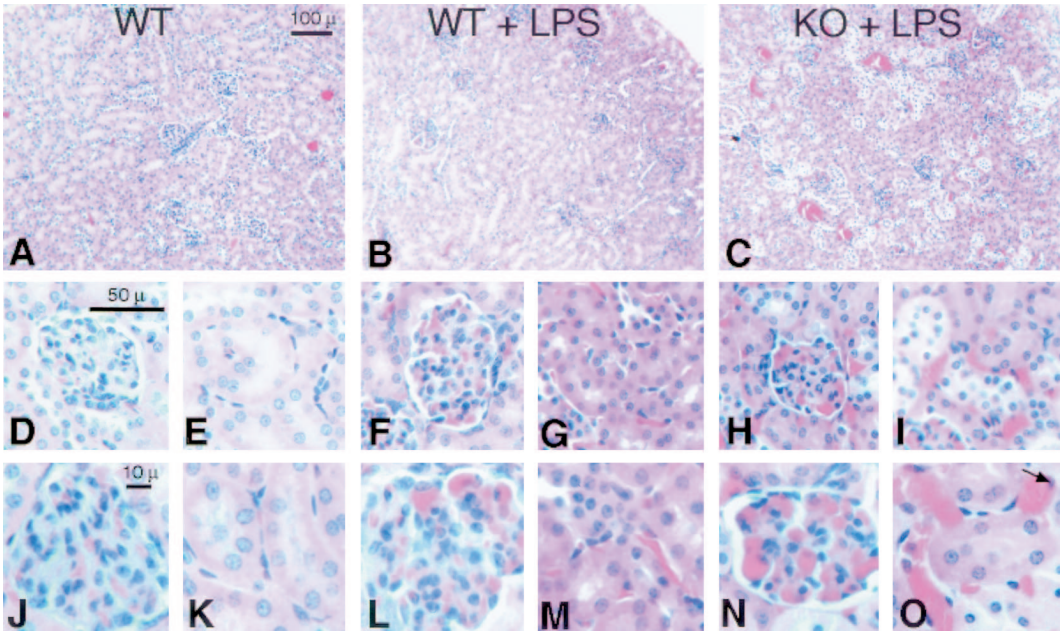

Figure 3. Renal vascular congestion and endothelial cell apoptosis occur in CD31-deficient mice following LPS stimulation. Representative low- (**A–C**) and high- (**D–O**) power H&E micrographs of kidneys harvested from age- and sex-matched wild-type control mice (WT), wild-type mice treated with LPS (WT + LPS), and CD31-deficient mice treated with LPS (KO + LPS). Kidney tissue harvested from CD31-deficient mice (not shown) appeared indistinguishable from WT control mice (**A, D**, **E**, **J**, and **K**). Treatment of WT mice with LPS resulted in modest glomerular and peri-tubular capillary congestion (compare **D**, **E**, **J**, and **K** with **F**, **G**, **L**, and **M**). In contrast, treatment of CD31-deficient mice with LPS resulted in significant glomerular and peri-tubular capillary vascular congestion and pyknosis of peri-tubular capillary endothelial cell nuclei (**arrow**) (**H**, **I**, **N,** and **O**). **Bar**, 100 μm (**A–C**); **bar**, 50 μm (**D–I**); **bar**, 10 μm (**J** to **O**).

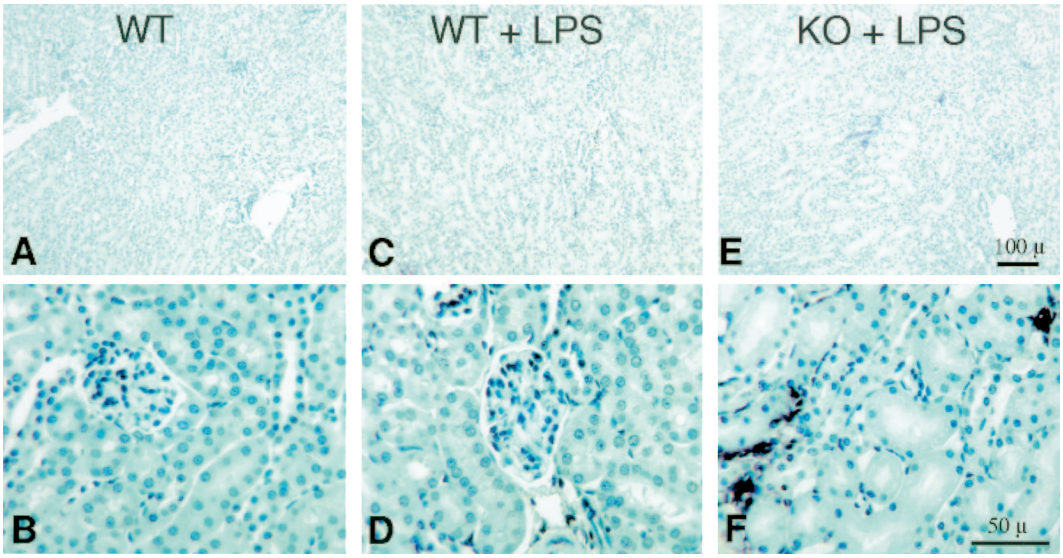

Figure 4. Renal peri-tubular capillary endothelial cell apoptosis occurs in CD31-deficient mice following LPS stimulation. Representative low- (**A**, **C**, and **E**) and high- (**B**, **D**, and **F**) power micrographs TUNEL-stained sections of kidneys harvested from age- and sex-matched wild-type control mice (WT), wild-type mice treated with LPS (WT + LPS), and CD31-deficient mice treated with LPS (KO + LPS). Kidney tissue harvested from CD31-deficient mice (not shown) appeared indistinguishable from WT control mice having no TUNEL positivity (**A** and **B**). Treatment of WT mice with LPS yielded no TUNEL positivity (compare **A** and **B** with **C** and **D**). In contrast, treatment of CD31-deficient mice with LPS resulted in significant TUNEL positivity of peri-tubular capillary endothelial cell nuclei (**E** and **F**). **Bar**, 100 μm (**A**, **C**, and **E**); **bar**, 50 μm (**B**, **D**, and **F**).

A time-course study over a 24-hour period following LPS treatment revealed increases in several other cytokines including IFNγ, MCP-1, MCP-5, IL-6, and sTNFR1 (Figure 7B).

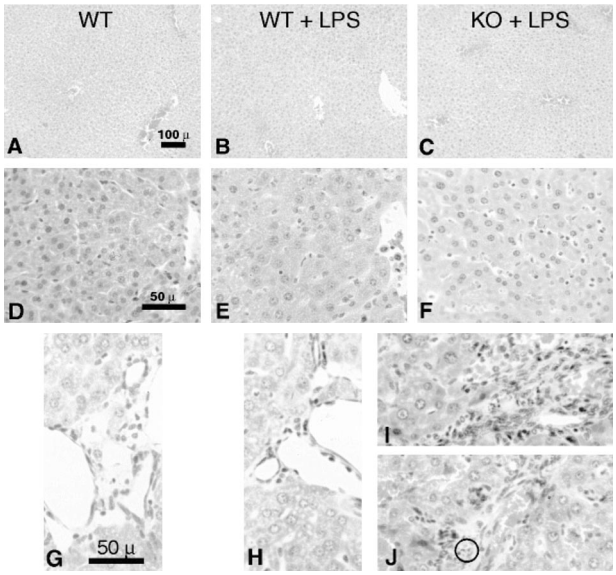

Figure 5. Hepatic vascular congestion and sinusoidal neutrophilic infiltration and apoptosis occur in CD31-deficient mice following LPS stimulation. Representative low- (**A** to **C**) and high- (**D** to **F**) power H&E micrographs of livers harvested from age- and sex-matched wild-type control mice (WT), wild-type mice treated with LPS (WT + LPS), and CD31-deficient mice treated with LPS (CD31 + LPS). Liver tissue harvested from CD31-deficient mice (not shown) appeared indistinguishable from WT control mice (**A**, **D**, and **G**). Treatment of WT mice with LPS resulted in very modest hepatic vascular and sinusoidal congestion (compare **A**, **D**, and **G** with **B**, **E**, and **H**). In contrast, treatment of CD31-deficient mice with LPS resulted in significant hepatic vascular and sinusoidal congestion, sinusoidal neutrophilic infiltration (**C** and **F**), and portal monocytic and neutrophilic infiltration (**I** and **J**) with occasional neutrophilic apoptosis (**J**, **circle**). **Bar**, 100 μm (**A–C**); **bar**, 50 μm (**D–F**); **bar**, 50 μm (**G–J**).

Reduced STAT3 Phosphorylation in Spleens and Cultured Splenic Lymphocytes from LPS-Treated CD31-Deficient Mice

One day (24 hours) following a 200-mg dose of LPS, spleens were harvested from wild-type and CD31-deficient mice. Splenic lysates run on 8% SDS PAGE and pSTAT3 levels determined following normalization to total

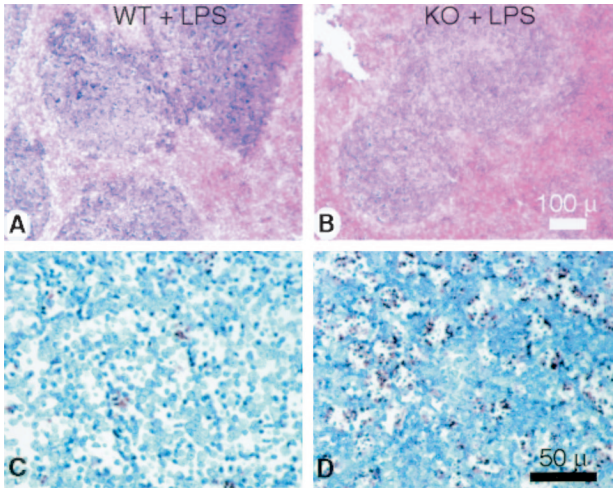

Figure 6. Splenic congestion and apoptosis occurs in CD31-deficient mice following LPS stimulation. **A** and **B:** Representative low-power micrographs of spleens from age- and sex-matched wild-type (WT) and CD31-deficient mice (KO + LPS) treated with LPS. LPS treatment elicited significantly more congestion in the red pulp of spleens of the KO mice. **Bar**, 100 μm. **C** and **D:** Peroxidase-labeled micrographs of sections of splenic tissue from WT (**C**) and CD31 KO (**D**) animals stained with TUNEL reagent. A robust increase in TUNEL labeling was noted in CD31 KO animals following treatment with LPS while no appreciable increase in TUNEL labeling was noted in WT animals. **Bar**, 50 μm (representative of four experiments).

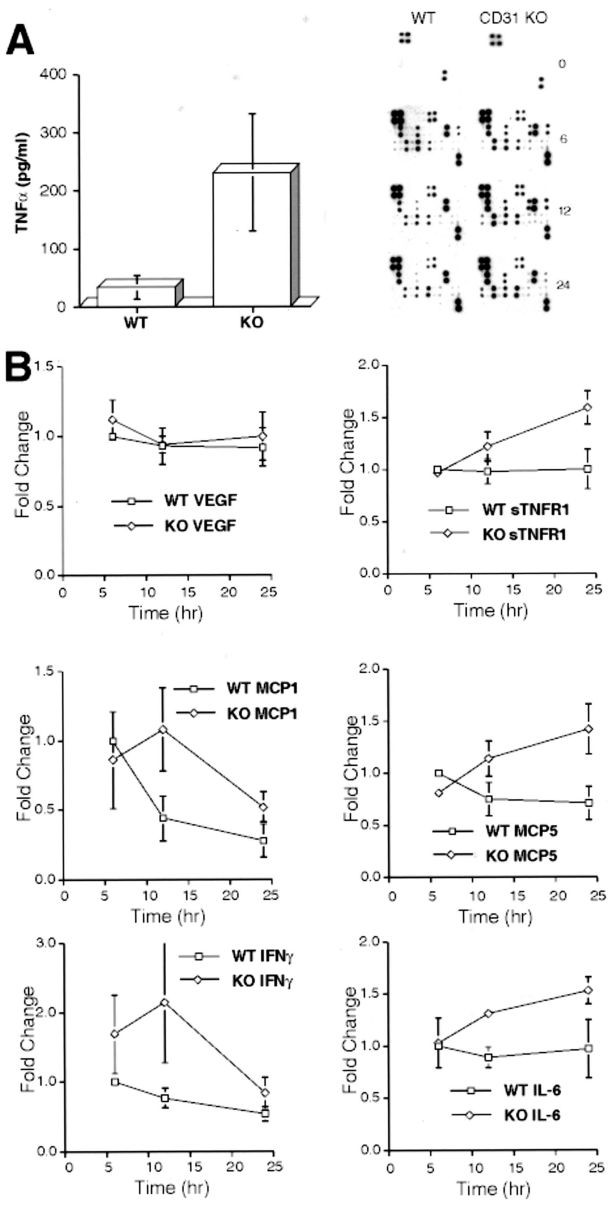

Figure 7. LPS treatment elicits significant increases in TNFα and other selected cytokine serum levels in CD31-deficient mice compared to WT mice. **A:** ELISA assays showed approximately a 10-fold increase in TNFα levels in the sera of CD31-deficient mice (233 pg/ml) compared to WT mice (25 pg/ml), $n = 8$, $P < 0.003$. **B:** Higher levels of several cytokines including INFγ, IL-6, MCP-1, MCP-5, and sTNFR1 were noted when sera was assayed using a Panomics cytokine array assay to assess cytokine profiles over a 24-hour time period of WT and CD31 KO animals treated with LPS. Other cytokines (VEGF [shown] and TPO, TARC, SCF, RANTES, MIP-3B, MIP-2, MIP-1A, LEPTIN, KC, IL-9, IL-5, IL-4, IL-3, IL-2, IL-17, IL-13, IL-12, IL-10, GMCSF, GCSF, EOTAXIN, CTACK, and 6CKINE [not shown]) similarly assessed did not exhibit any appreciable changes in response to LPS. Data were accrued from three independent experiments, each run in duplicate. Results were confirmed using the BD cytodex bead assay (not shown). A representative series of cytokine arrays illustrating the differences between the sera harvested from WT and CD31 KO animals following LPS treatment is included.

STAT3. As illustrated in Figure 8, spleens harvested from CD31-deficient animals exhibited significantly lower pSTAT3 levels compared to those harvested from LPS-treated wild-type mice ($P = 0.004$) (Figure 8A). Similarly, following a 24-hour treatment with 10 ng/ml or 100 ng/ml of LPS, purified splenocytes (T and B lymphocytes) harvested from CD31-deficient spleens also displayed reduced pSTAT levels compared to splenocytes harvested from wild-type mice (Figure 8B).

Immunofluorescence staining of frozen sections of splenic tissue harvested from control and LPS-treated (200 μg for 12 hours) WT and CD31 KO mice revealed a 3.7-fold increase ($P < 0.04$) in pSTAT3-labeled nuclei in WT spleens following LPS treatment, while no appreciable change (0.94, $P = 0.5$) in nuclear localization of pSTAT3 was noted in CD31 KO mice (Figure 8, C to F).

Immunofluorescence staining of frozen sections of splenic tissue harvested from control and LPS-treated (200 μg for 12 hours) WT and CD31 KO mice double-labeled with anti-Mac-3, to identify splenic macrophages and monocytes, and anti-pSTAT3 revealed essentially no appreciable differences in macrophage/monocyte numbers (green fluorescence) and macrophage pSTAT3 cellular localization patterns (red fluorescence) among WT and CD31-deficient mice before and following LPS treatment (Figure 8, G to J) at the time point studied. Essentially no nuclear pSTAT3 localization was appreciated in Mac-3-positive cells in both WT and KO spleens harvested from control and LPS-treated animals at the 12-hour time point.

Decreased STAT3 Phosphorylation and Nuclear Localization in Response to LPS in Immortalized Pulmonary Endothelial Cells from CD31-Deficient Mice

Endothelial cells are known to express Toll receptors on their surfaces.[22] To assess the effects of CD31 on TLR4 signaling, immortalized lung microvascular endothelial cells, derived from CD31-deficient mice and these cells stably transfected and expressing full-length CD31, were incubated with LPS at a concentration of 100 ng/ml for 0.5, 2, 6, 12 and 24 hours. Cells were then stained for STAT3 and pSTAT3 expression levels and localization. As illustrated in Figure 9, A and B, the CD31-deficient endothelial cells exhibited significantly reduced pSTAT3 levels in the absence and presence of 100 ng/ml LPS. Further, at each time point examined during a 12-hour time course, the CD31-deficient endothelial cells exhibited significantly reduced pSTAT3 levels compared to the cells stably transfected and expressing full-length CD31, although their total STAT3 levels were essentially identical (*, $P < 0.05$).

In addition to exhibiting reduced levels of pSTAT3 in response to LPS treatment, the PECAM-1-deficient endothelial cells demonstrated minimal pSTAT3 nuclear translocation as opposed to the PECAM-1 reconstituted cells, which exhibited significant nuclear localization of pSTAT3 when assessed by immunofluorescence microscopy (Figure 9, C to F).

IL-6 Stimulation of PECAM-1 Expressing Splenic Lymphocytes Elicits Increased Expression of pSTAT3 Compared to PECAM-1-Deficient Cells and Sodium Orthovanadate Inhibition of Phosphatase Activity in IL-6-Stimulated Splenic Lymphocytes Elicits Increased Phosphorylation of STAT3 in CD31-Deficient Cultures

Splenic lymphocyte cultures derived from WT and KO spleens were stimulated with IL-6 (1 ng/ml) for 15 to 30 minutes in the absence and presence of sodium orthovanadate. In the absence of sodium orthovanadate, Western blot analyses of lysates revealed marked decreases in STAT3 phosphorylation in the IL-6 stimulated CD31-deficient lymphocyte cultures compared to wild-type cultures. Interestingly, in the presence of sodium orthovanadate, the levels of pSTAT3 in the IL-6-stimulated CD31-deficient lymphocyte cultures were found to be similar to the levels observed in similarly treated wild-type cultures (Figure 10).

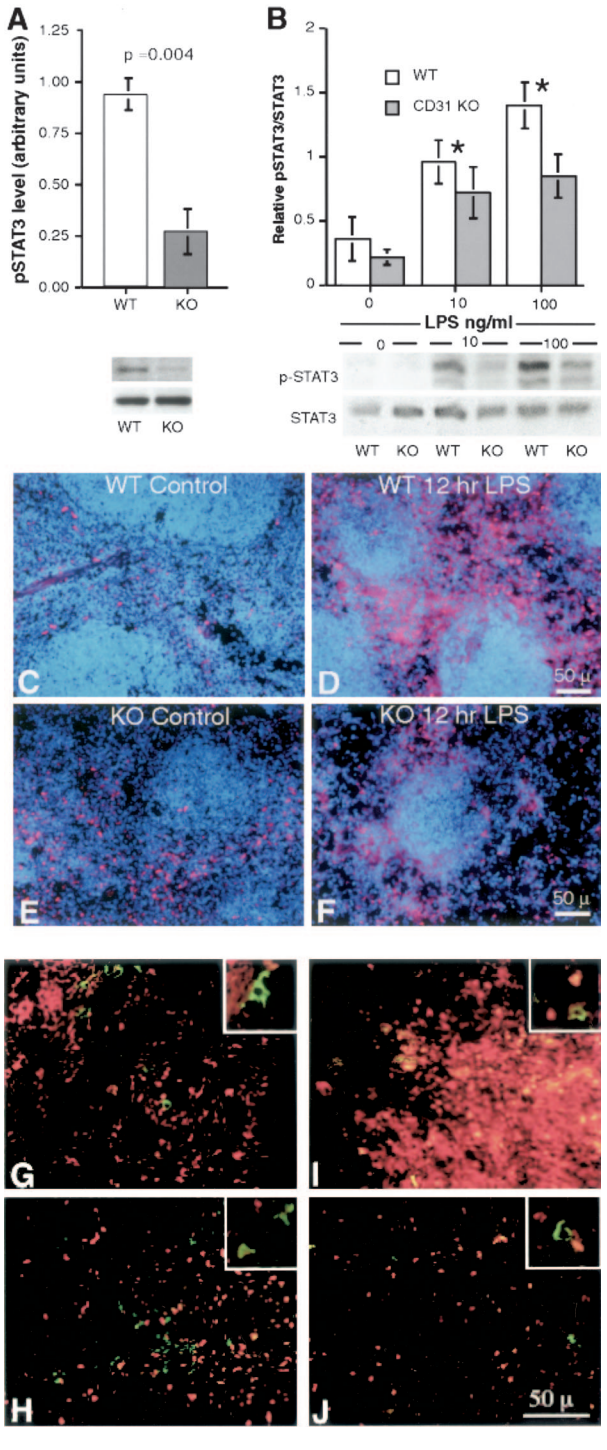

Figure 8. Splenic lysates and splenic lymphocytes harvested from CD31-deficient mice exhibit decreased pSTAT3 levels compared to WT mice following LPS stimulation. **A:** The **top** panel represents quantitation of the relative pSTAT3 levels (sex- and age-matched averages of five and five CD31 KO animals treated with LPS and harvested 24 hours later) of splenic tissue harvested from wild-type (WT) and CD-31-deficient (CD31 KO) animals, normalized to total STAT3 ($P < 0.004$). The KO spleens exhibit a 75% decrease in pSTAT3 compared to WT spleens. The **bottom** panel is a representative Western blot of pSTAT3 and STAT3 from one WT and one CD31 KO animal of the group tested. **B:** The **top** panel represents the quantitation of the relative pSTAT3 levels of lymphocytes harvested from the spleens of WT and KO mice and cultured *in vitro* for 24 hours in the absence and presence of 10 and 100 ng/ml LPS. The lymphocytes harvested from CD31 KO spleens exhibit a significant decrease in pSTAT3 compared to WT splenic lymphocytes in the absence of LPS and at both LPS concentrations, normalized to total STAT3. The **bottom** panel is a Western blot of pSTAT3 and STAT3 from the lymphocytes harvested from a WT and a CD31 KO animal. **C–F:** Immunofluorescence micrographs of 6-μm frozen sections of splenic tissue from WT (**C**) and CD31-deficient (KO) (**D**) animals stained with pSTAT3 (red fluorescence) and DAPI (blue fluorescence). A 3.7-fold increase ($P < 0.04$) in pSTAT3 labeling was noted in WT animals following treatment with LPS (compare **C** and **D**) while no appreciable increase in pSTAT3 labeling was noted in CD31 KO animals (0.95, $P = 0.45$) (compare **E** and **F**) (representative of three experiments). **G- J:** Immunofluorescence micrographs of 6-μm frozen sections of splenic tissue from WT (**G** and **I**) and CD31-deficient (KO) (**H** and **J**) animals stained with pSTAT3 (red fluorescence) and Mac-3 (green fluorescence) revealed essentially no differences in macrophage pSTAT3 localization before (**G** and **H**) or following (**I** and **J**) LPS treatment. The increased pSTAT3 nuclear expression noted in the WT LPS sample (**I**) is manifested as red to yellow fluorescence due to the intensity of the fluorescence. Essentially no nuclear pSTAT3 localization was appreciated in Mac-3-positive cells as evidenced by the lack of any pSTAT3 nuclear staining in the cells expressing green fluorescence in their cytoplasm (**insets**).

TLR4 Expression in Splenocytes, Splenic Lysates, Endothelial Cells, and Endothelial Cell Lysates from WT and CD31-Deficient Mice Is Essentially Unchanged

In an attempt to further elucidate the mechanism(s) underlying the observed differences in STAT3 subcellular localization and phosphorylation in WT and CD31-deficient mice, splenocytes from WT and CD31-deficient mice were analyzed for surface TLR4 expression by FACS analysis and Western blotting. FACS analysis revealed no appreciable changes in TLR4 expression on splenocytes and endothelial cells isolated from WT or CD31-deficient animals in the absence or presence of LPS (Figure 11). These results were confirmed by Western blot analysis of TLR4 expression (data not shown).

Discussion

We here demonstrated that CD31 modulates the systemic response to LPS and prevents the development of septic shock by at least three mechanisms: maintenance

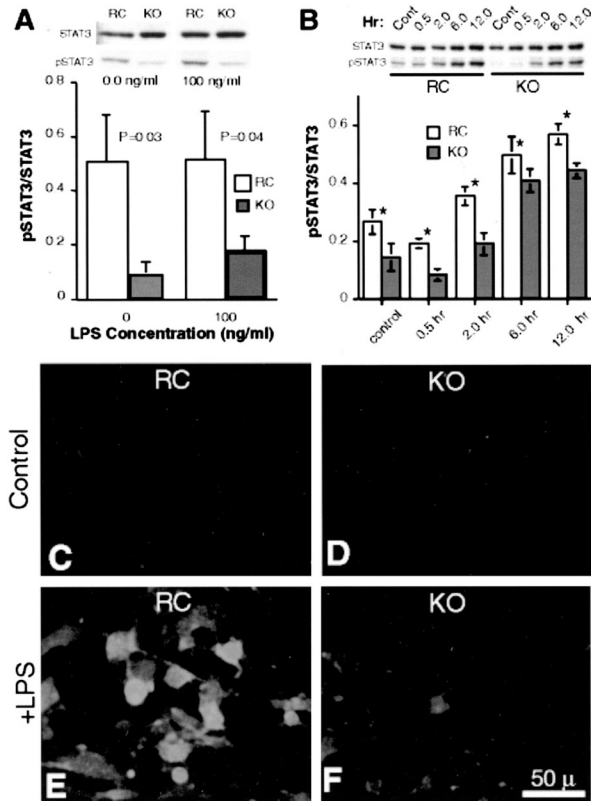

Figure 9. Immortalized pulmonary endothelial cells derived from CD31-deficient mice exhibit decreased levels of p-STAT3 in response to LPS exposure *in vitro*. **A: Top**, representative Western blot of KO lung endothelial cells revealed decreased levels of pSTAT3 compared to PECAM-1-reconstituted cells (RC), although both cell types expressed approximately equal amounts of total STAT3. Following stimulation with 100 ng/ml LPS, unlike the increases noted in the RC cells, the KO cells exhibited a significantly blunted pSTAT3 response. **Bottom**, average of five independent experiments illustrating the blunted pSTAT3 response in KO cells (*****, $P < 0.0$ 5). **B:** Western blot analysis of KO lung endothelial cells and PECAM-1-reconstituted cells stimulated with 100 ng/ml LPS over a 12-hour time period revealed decreased levels of pSTAT3 in KO endothelial cells compared to PECAM-1-reconstituted (RC) endothelial cells, although both cell types expressed approximately equal amounts of total STAT3 ($n = 5$; *****, P value < 0.05). **C** to **F:** Immortalized pulmonary endothelial cells derived from CD31-deficient mice exhibit decreased nuclear localization of pSTAT3 in response to LPS exposure *in vitro*. Immunofluorescence microscopy of cultured PECAM-1-reconstituted endothelial cells (RC) (**C** and **E**) and KO endothelial cells (**D** and **F**) in the absence (**C** and **D**) and presence (**E** and **F**) of LPS revealed no appreciable nuclear localization of pSTAT3 in both cell types in the absence of LPS (**C** and **D**). In contrast, the presence of nuclear pSTAT3 was noted in RC cells but was significantly reduced in KO cells following LPS treatment (**E** and **F**). **Bar**, 50 μm.

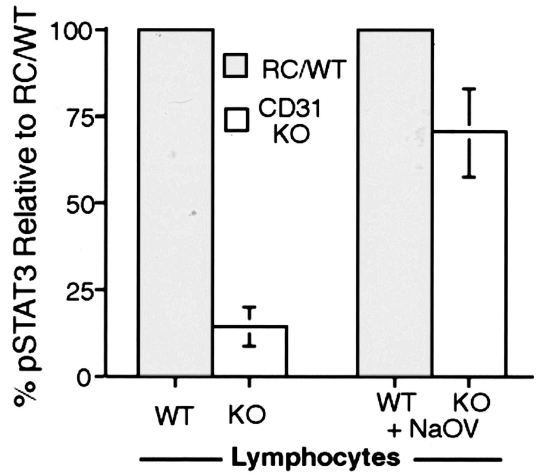

Figure 10. IL-6 stimulation of PECAM-1 expressing splenic lymphocytes elicits increased expression of pSTAT3 and sodium orthovanadate inhibition of phosphatase activity in IL-6 stimulated splenic lymphocytes elicits increased phosphorylation of STAT3 in CD31-deficient cultures. WT and KO splenic lymphocyte cultures were stimulated with IL-6 (1 ng/ml) for 15 to 30 minutes in the absence (WT and KO lymphocytes) and presence of Sodium orthovanadate (WT and KO lymphocytes + NaOV). In the absence of sodium orthovanadate, Western blot analyses of lysates revealed marked decreases in STAT3 phosphorylation in the IL-6 stimulated CD31-deficient lymphocyte cultures (**open bars**) compared to wild-type cultures (**shaded bars**). In the presence of sodium orthovanadate, the levels of pSTAT3 in the IL-6 stimulated CD31-deficient lymphocyte cultures were found to be similar to the levels observed in similarly treated wild-type cultures (averages of two independent experiments).

of endothelial integrity, modulation of STAT3 phosphorylation, and modulation of apoptosis.

A prior study in the mouse EAE model revealed that initiation of central nervous system (CNS) inflammation in CD31-deficient mice caused enhanced, prolonged breakdown of the blood-brain endothelial barrier as compared to wild-type mice.[12] These changes led to increased CNS vascular permeability and earlier onset of clinical disease. Similar to the findings in EAE, we here showed that a systemic inflammatory challenge with LPS also causes enhanced vascular leak in CD31-deficient mice that contributes to increased mortality.

As determined by the Evans Blue technique and histopathology of lung, liver, and kidney, this alteration of endothelial integrity occurred within 24 hours of an LPS challenge. This role for CD31 is, therefore, not specific to the blood-brain endothelial barrier, and its expression in other solid organs appears necessary to prevent severe inflammatory injury. Its effects also appear to be important very early in the inflammatory response. In immediate hypersensitivity reactions induced by histamine, CD31-deficient mice and cultured endothelial cells exhibit prolonged permeability changes compared to wild-type cells.[12]

These results are consistent with the hypothesis that CD31 is involved in the timely restoration of interendothelial junctional integrity following an inflammatory stimulus but is not necessary for maintenance of endothelial integrity in the normal quiescent state.[10,23] Although CD31 also mediates leukocyte adhesion and facilitates transendothelial migration in some vascular beds, other adhesion molecules appear to compensate for the absence of CD31 in knockout animals. Further, its effects on vascular integrity do not appear to be duplicated by other molecules.

In addition to changes in vascular permeability, we also observed impaired phosphorylation of STAT3 in CD31-deficient mice and cultured splenocytes and endothelial cells. The regulation of the APR by STAT3 is complex because it mediates transcription of pro- and anti-inflammatory genes.[19,20] However, work in cell-specific knockout mice suggests that its anti-inflammatory effects are physiologically dominant and are important in the termination of the APR. Mice deficient in STAT3 in macrophages and neutrophils demonstrate increased mortality in LPS-induced shock associated with increased production of pro-inflammatory cytokines such as TNF-α and IL-6.[20] Macrophages and neutrophils from

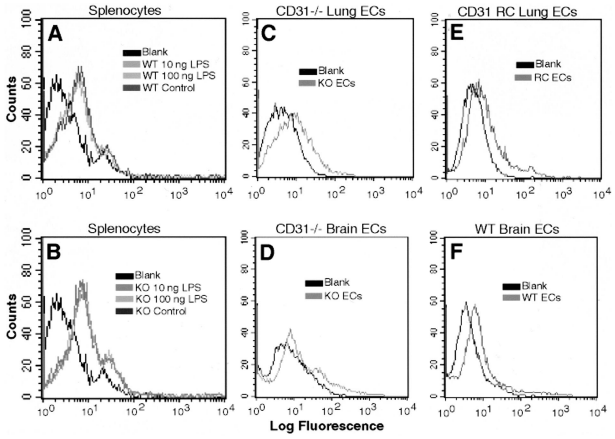

Figure 11. TLR4 expression of WT and CD31-deficient splenocytes and endothelial cells remains constant and does not change following LPS treatment. Representative FACS analyses of WT (**A**) and KO (**B**) splenocytes in the absence and presence of LPS; KO (**C**) and PECAM-1 reconstituted (**D**) lung endothelial cells and KO (**E**) and WT (**F**) brain endothelial cells illustrating essentially no differences in TLR4 expression. This was confirmed by Western blot analyses (data not shown).

these mice are not responsive to the immune-suppressive cytokine, IL-10. In STAT3-deficient hepatocytes, LPS does not induce a subset of IL-6-responsive, acute phase genes that may be important in recovery from endotoxic shock.[19] Our findings of dysregulated cytokine induction in PECAM-1-deficient mice following LPS challenge are consistent with the data presented in this report and our previous data,[8,24] suggesting that PECAM-1 serves as a scaffolding on which STAT isoforms are differentially phosphorylated, providing a regulatory mechanism of STAT signaling; and on which the phosphatase SHP-2, known to be involved in IL-6 signaling, can be sequestered, modulating its activity. Indeed, inhibition of phosphatase activity (by sodium orthovanadate) during IL-6 stimulation of lymphocytes elicits a blunting of the dephosphorylation of pYSTAT3 in CD31 KO splenocytes, resulting in pSTAT3 levels in the CD31 KO splenocytes that more closely approximate those of the WT splenocytes (% pSTAT3 relative to WT = 14.3% ± 5.56 without sodium orthovanadate versus 70.1% ± 13 with the addition of sodium orthovanadate) (Figure 10). Thus, we hypothesize that CD31-mediated regulation of endothelial integrity and STAT3 phosphorylation state occur through its role as a scaffolding molecule (Figure 12).

Junctional complexes formed by transmembrane molecules including as VE-cadherin maintain endothelial integrity and associate with the cellular cytoskeleton through the intracellular protein β-catenin. Many vasoactive agents are known to elicit tyrosine phosphorylation of several junctional components including β-catenin. This phosphorylation leads to dissociation of VE-cadherin and β-catenin and to breakdown of the adherens junctional complex. CD31 binds tyrosine phosphorylated β-catenin and stimulates its dephosphorylation by also binding the phosphatase SHP-2, thus serving as a scaffolding, bringing both the tyrosine phosphorylated β-catenin and SHP-2 into close proximity and facilitating the dephosphorylation of the phosphorylated β-catenin.[6,7,10,24] The dephosphorylated β-catenin would then be available to bind VE-cadherin which leads to the reassembly of the junctional complex and barrier integrity.[6–8]

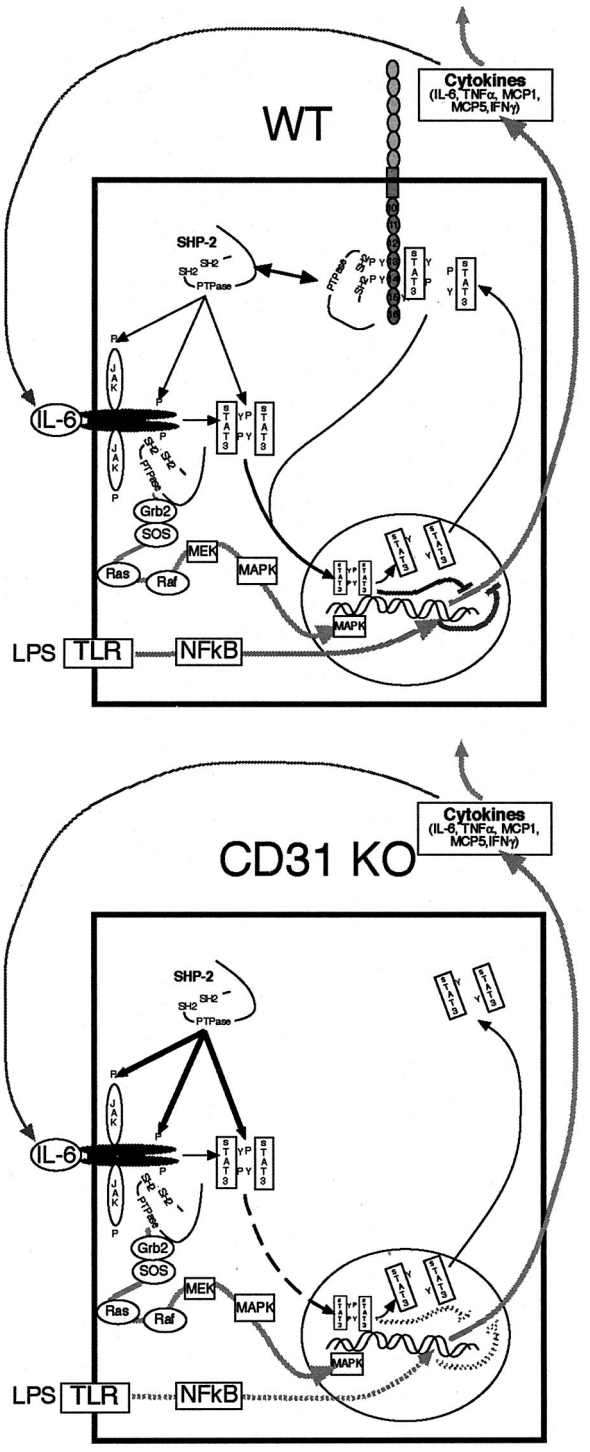

Figure 12. Current working model of the role of PECAM-1 as a modulator of cytokine expression. PECAM-1 facilitates down-regulation of LPS-induced IL-6-mediated cytokine induction by modulating the localization and activities of SHP-2 (WT). In the absence of PECAM-1, SHP-2 binds and dephosphorylates STAT3 rendering it unable to translocate to the nucleus and initiate the down-regulation of cytokine expression, which may potentiate sustained cytokine expression in CD31 KO animals.

Additionally, CD31 also facilitates the phosphorylation of STAT3. STAT3 in its dephosphorylated form is thought to bind to the cytoplasmic tail of CD31 and become tyrosine phosphorylated there by an undefined kinase which binds to the Y686 ITAM tyrosine.[8,10] Phosphorylated STAT3 would then dissociate from the complex and be transported to the nucleus to regulate gene transcription. This model suggests that CD31 functions as a reservoir/binding site for sequestration, activation, and/or phosphorylation/dephosphorylation of molecules such as β-catenin, FAK, SHP-2, and STAT3.[6–8,10,24,25] Exactly how this dynamic binding and activation occurs temporally following an inflammatory stimulus remains unclear but differential phosphorylation/dephosphorylation of the PECAM-1 ITAM tyrosines Y663 and Y686 and selected serine residues have been shown to be involved.[6–8,9,10,23,24]

Additionally, we have found that splenocytes, splenic tissue, and cultured endothelial cells harvested from CD31-deficient mice exhibit no appreciable changes in TLR4 expression compared to WT cells and tissues (Figure 11).

Our findings of increased splenocyte, endothelial cell, and PMN apoptosis in tissues and cells derived from PECAM-1-deficient mice following LPS treatment is consistent with published findings.[10,11,26–29] Several of PECAM-1's known binding partners including β- and γ-catenin, SHP-2, and STAT3 and 5 are known to be involved in apoptotic and cell survival signaling pathways.[9] These data suggest that PECAM-1 may serve as a modulator of apoptotic/survival pathways via its scaffolding/binding properties, perhaps being regulated by differential tyrosine and serine phosphorylation/dephosphorylation.

Within the context of its ability to participate in the maintenance endothelial integrity, the modulation of STAT3 phosphorylation and apoptosis, CD31 can be considered as a negative regulator of systemic and organ-specific inflammatory responses (Figure 12). Its role is independent of the nature of the initial immune stimulus. It can be induced systemically by an innate immune stimulus such as LPS or by an organ-specific autoimmune response initiated by the adaptive immune system as in EAE. Additional work is required to elucidate the independent and possibly interdependent roles of CD31-mediated regulation of SHP-2, β-catenin, and STAT3 during inflammation.[10,30] Since selected kinases and phosphatases bind to CD31 through its ITAM domain, modulation of tyrosine phosphorylation of this domain represents a potential therapeutic target, and further study is needed to determine the feasibility of that approach.

Acknowledgments

We thank Dr. Charles Janeway for his support.

References

1. Newman P, Berndt MC, Gorski J, White GC, Lyman S, Paddock C, Muller WA: PECAM-1 (CD31) cloning and relation to adhesion molecules of the immunoglobulin gene family. Science 1990, 247: 1219–1222
2. Muller W, Ratti C, McDonnell S, Cohn Z: A human endothelial cell-restricted, externally disposed plasmolemmal protein enriched in intercellular junctions. J Exp Med 1989, 170:399–414
3. Abelda S, Oliver P, Romer L, Buck C: EndoCAM: a novel endothelial cell-cell adhesion molecule. J Cell Biol 1990, 110:1227–1237
4. Ohto H, Maeda H, Shibata Y, Chen RF, Ozaki Y, Higashihara M, Takeuchi A, Tohyama H: A novel leukocyte differentiation antigen: two monoclonal antibodies TM2 and TM3 define a 120-kd molecule present on neutrophils, monocytes, platelets, and activated lymphoblasts. Blood 1985, 66:873–881
5. Stockinger H, Gadd SJ, Eher R, Majdic O, Schreiber W, Kasinrerk W, Strass B, Schnabl E, Knapp W: Molecular characterization and functional analysis of the leukocyte surface protein CD31. J Immunol 1990, 145:3889–3897
6. Ilan N, Mahooti S, Rimm DL, Madri JA: PECAM-1 (CD31) functions as a reservoir for and a modulator of tyrosine-phosphorylated beta-catenin. J Cell Sci 1999, 112:3005–3014
7. Ilan N, Cheung L, Pinter E, Madri JA: Platelet-endothelial cell adhesion molecule-1 (CD31), a scaffolding molecule for selected catenin family members whose binding is mediated by different tyrosine and serine/threonine phosphorylation. J Biol Chem 2000, 275:21435–21443
8. Ilan N, Cheung L, Miller S, Mohsenin A, Tucker A, Madri JA: Pecam-1 is a modulator of stat family member phosphorylation and localization: lessons from a transgenic mouse. Dev Biol 2001, 232:219–232
9. Newman PJ, Newman DK: Signal transduction pathways mediated by PECAM-1: new roles for an old molecule in platelet and vascular cell biology. Arterioscler Thromb Vasc Biol 2003, 23:953–964
10. Ilan N, Madri JA: PECAM-1: old friend, new partners. Curr Opin Cell Biol 2003, 15:515–524
11. Muller W, Weigl S, Deng X, Phillips D: PECAM-1 is required for transendothelial migration of leukocytes. J Exp Med 1993, 178:449–460
12. Graesser D, Solowiej A, Bruckner M, Osterweil E, Juedes A, Davis S, Ruddle NH, Engelhardt B, Madri JA: Altered vascular permeability and early onset of experimental autoimmune encephalomyelitis in PECAM-1-deficient mice. J Clin Invest 2002, 109:383–392
13. Nathan C: Points of control in inflammation. Nature 2002, 420:846–852
14. Janeway Jr CA, Medzhitov R: Innate immune recognition. Annu Rev Immunol 2002, 20:197–216
15. Cohen J: The immunopathogenesis of sepsis. Nature 2002, 420:885–891
16. Pasare C, Medzhitov RS: Toll pathway-dependent blockade of CD4+CD25+ T cell-mediated suppression by dendritic cells. Science 2003, 299:1033–1036
17. Akira S, Nishio Y, Inoue M, Wang X, Wei S, Matsusaka T, Yoshida K, Sudo T, Naruto M, Kishimoto T: Molecular cloning of APRF, a novel IFN-stimulated gene factor 3 p91-related transcription factor involved in the gp130-mediated signaling pathway. Cell 1994, 77:63–71
18. Zhong Z, Wen Z, Darnell Jr JE: Stat3: a STAT family member activated by tyrosine phosphorylation in response to epidermal growth factor and interleukin-6. Science 1994, 264:95–98
19. Alonzi T, Maritano D, Gorgoni B, Rizzuto G, Libert C, Poli V: Essential role of STAT3 in the control of the acute-phase response as revealed by inducible gene activation in the liver. Mol Cell Biol 2001, 21:1621–1632
20. Takeda K, Clausen BE, Kaisho T, Tsujimura T, Terada N, Forster I, Akira S: Enhanced Th1 activity and development of chronic enterocolitis in mice devoid of Stat3 in macrophages and neutrophils. Immunity 1999, 10:39–49
21. Duncan G, Andrew DP, Takimoto H, Kaufman SA, Yoshida H, Spellberg J, Luis de la Pompa J, Elia A, Wakeham A, Karan-Tamir B, Muller WA, Senaldi G, Zukowski MM, Mak TW: Genetic evidence for functional redundancy of platelet/endothelial cell adhesion molecule-1 (PECAM-1): CD31-deficient mice reveal PECAM-1-dependent and PECAM-1-independent functions. J Immunol 1999, 162:3022–3030
22. Faure E, Thomas L, Xu H, Medvedev A, Equils O, Arditi M: Bacterial lipopolysaccharide and IFN-gamma induce Toll-like receptor 2 and Toll-like receptor 4 expression in human endothelial cells: role of NF-kappa B activation. J Immunol 2001, 166:2018–2024
23. Payne GW, Madri JA, Sessa WC, Segal SS: Histamine inhibits conducted vasodilation through NO production in arterioles of mouse skeletal muscle. FASEB J 2004, 18:280–286

24. Gratzinger D, Barreuther M, Madri JA: Platelet-endothelial cell adhesion molecule-1 modulates endothelial migration through its immunoreceptor tyrosine-based inhibitory motif. Biochem Biophys Res Commun 2003, 301:243–249
25. Gratzinger D, Canosa S, Engelhardt B, Madri JA: Platelet endothelial cell adhesion molecule-1 modulates endothelial cell motility through the small G-protein Rho. FASEB J 2003, 17:1458–1469
26. You M, Flick LM, Yu D, Feng G-S: Modulation of the nuclear factor kB pathway by Shp-2 tyrosine phosphatase in mediating the induction of interleukin (IL)-6 by IL-1 or tumor necrosis factor. J Exp Med 2001, 193:101–109
27. Gao C, Sun W, Christofidou-Solomidou M, Sawada M, Newman DK, Bergom C, Albelda SM, Matsuyama S, Newman PJ: PECAM-1 functions as a specific and potent inhibitor of mitochondrial-dependent apoptosis. Blood 2003, 102
28. Ferrero E, Belloni D, Contini P, Foglieni C, Ferrero ME, Fabbri M, Poggi A, Zocchi MR: Transendothelial migration leads to protection from starvation-induced apoptosis in CD34+CD14+ circulating precursors: evidence for PECAM-1 involvement through Akt/PKB activation. Blood 2003, 101:186–193
29. Brown S, Heinisch I, Ross E, Shaw K, Buckley CD, Savill J: Apoptosis disables CD31-mediated cell detachment from phagocytes promoting binding and engulfment. Nature 2002, 418:200–203
30. Biswas P, Canosa S, Schoenfeld J, Schoenfeld D, Tucker A, Madri JA: PECAM-1 promotes beta-catenin accumulation and stimulates endothelial cell proliferation. Biochem Biophys Res Commun 2003, 303:212–218